Tropospheric Scintillation With Concurrent Rain Attenuation at 50 GHz in Madrid

Pedro Garcia-del-Pino, José Manuel Riera, and Ana Benarroch

Abstract—**Tropospheric scintillation can become a significant impairment in satellite communication systems, especially in those with low fade-margin. Moreover, fast amplitude fluctuations due to scintillation are even larger when rain is present on the propagation path. Few studies of scintillation during rain have been reported and the statistical characterization is still not totally clear. This paper presents experimental results on the relationship between scintillation and rain attenuation obtained from slant-path attenuation measurements at 50 GHz. The study is focused on the probability density function (PDF) of various scintillation parameters. It is shown that scintillation intensity, measured as the standard deviation of the amplitude fluctuations, increases with rain attenuation; in the range 1–10 dB this relationship can be expressed by power-law or linear equations. The PDFs of scintillation intensity conditioned to a given rain attenuation level are lognormal, while the overall long-term PDF is well fitted by a generalized extreme value (GEV) distribution. The short-term PDFs of amplitude conditioned to a given intensity are normal, although skewness effects are observed for the strongest intensities. A procedure is given to derive numerically the overall PDF of scintillation amplitude using a combination of conditional PDFs and local statistics of rain attenuation.**

I. Introduction

THE troposphere structure and composition affect the propagation of millimeter waves in satellite links [1], [2]. In particular, tropospheric scintillation, which is caused by small-scale fluctuations of the refractive index due to turbulence, produces random fades and enhancements of the received signal amplitude. Although rain and cloud attenuation are usually the most important factors that produce degradation in Earth–satellite links, scintillation can become a significant impairment in low-margin communication systems. Furthermore, when rain is present on the propagation path, the receiver experiences fast amplitude fluctuations superimposed on the slow variations caused by rain attenuation. A better characterization of these phenomena can be advantageous for the optimization of channel capacity in satellite links.

Clear-weather scintillation, or dry scintillation, has been widely characterized and modeled. There are numerous studies, both theoretical and empirical, of their effects on satellite links [3], [4]. Besides, some prediction models can be used to determine the amplitude fluctuations [2], [4], [5]. On the other hand, only a few studies of scintillation during rain, or wet scintillation, have been undertaken so far [6]–[8].

In the framework of a propagation experiment in the V-band carried out in Madrid, Spain, several atmospheric impairments, such as rain and cloud attenuation, were analyzed. The experiment consisted in measuring the 50-GHz beacon of the ITALSAT satellite for one year [9]. The main results concerning dry scintillation were published in [10].

The present analysis of wet scintillation data is focused on the characterization of the probability density function (PDF) of both scintillation intensity and amplitude fluctuations. The dependence of scintillation on rain attenuation is discussed, and results are compared with some theoretical models. The final objective is to obtain a set of expressions that can be used in the determination of the long-term distribution of scintillation amplitude.

A description of the measurement setup, including data analysis procedures, is given in Section II. Section III is devoted to review some theoretical models of scintillation. Measurement results and discussions about wet scintillation intensity are presented in Section IV. The main statistics of scintillation amplitude are dealt with in Section V, which also includes a method to derive the long-term distribution of scintillation amplitude. Conclusions are given in Section VI.

II. Experimental Details

A. Receiving System

The experimental station, installed on the premises of Universidad Politécnica de Madrid, consisted of a beacon receiver at 49.49 GHz and a radiometer at the same frequency. The centered Cassegrain antenna of 1.2 m diameter had a gain of 55 dBi and a global efficiency of about 81%. The elevation angle was 40°. A receiver margin of about 30 dB gave the possibility of analyzing most of the rain events at 50 GHz in a nontropical climate. The sampling rate of the measurements was 18.66 Hz, sufficient for a detailed study of tropospheric scintillation, whose power density is usually only significant for Fourier frequencies up to a few hertz. More details on the receiver performance and hardware features are given in [11].

A meteorological station near the antenna provided several surface parameters such as temperature, humidity, and wind

speed and direction. Rain intensity was measured with a tipping bucket rain gauge. Madrid is located in the central area of the Iberian Peninsula (40.27° N, 3.43° W), at an altitude of 630 m above sea level. It has a continental climate, with hot and dry summers and cold winters. Rain occurs mainly in spring and autumn, with the average rainfall being about 440 mm per year.

The receiver was designed to measure the two signal polarizations (horizontal and vertical) of the ITALSAT satellite beacon. Nevertheless, the following results are based on the analysis of the horizontally polarized signal, as scintillation is not expected to be significantly influenced by the polarization angle [12], [13].

B. Data Analysis

The experimental data set was divided into rain and non-rain periods. The beginning and end of each rain event were initially determined with the rain gauge data. However, a perfect separation between very low rain rate and no rain is not possible with a tipping-bucket rain gauge. For this reason, and also to account for the occurrence of attenuation caused by rain in the path that was not registered by the rain gauge, the intervals marked as rain periods have been extended to include several minutes before and after the beginning and end of rain events, as well as short inter-event intervals [9]. Thus, during a fraction of these periods marked as rainy, there is actually no precipitation, though clouds are usually present.

Visual inspection was performed on all data sequences to eliminate spurious and invalid data. A total of 150 precipitation events between January and December 2000 were processed and analyzed, totaling more than 570 hours, about 6.5% of the year. This is the data set used as experimental reference throughout this paper.

The scintillation contribution has been extracted from the time series of signal level using a fifth-order Butterworth high-pass filter. The cutoff frequency of this filter, 0.08 Hz, has been chosen after performing a spectral analysis. Fig. 1 shows the average power spectrum of eight time series collected during rain, totaling about 33 h; they were registered in May, which is usually one of the months with more convective events in Madrid. The theoretical −20 dB/decade slope due to rain [14] appears to be valid up to about 0.02–0.04 Hz. Beyond that point, there is a range in which rain and turbulence effects are superimposed. Then, the typical scintillation power spectrum becomes evident, showing a flat zone above 0.08–0.1 Hz and a final steep decay with a −80/3 dB/decade slope [15] down to the noise floor level. From the figure, it can be inferred that a cutoff frequency of 0.08 Hz allows to filter out most of the fast amplitude fluctuations due to rain, while keeping most of the scintillation components. This value is very close to the one found by other authors at the same frequency, 0.07 Hz [16].

After filtering out, the resulting data set consists of scintillation amplitudes, χ, i.e., positive (enhancement) and negative (fade) fluctuations above the mean level. From these data, scintillation intensity σ_χ is calculated as the standard deviation of the amplitude fluctuations in one-minute periods. The mean value of rain attenuation A is calculated from the original data every minute and related to the value of σ_χ in the same minute.

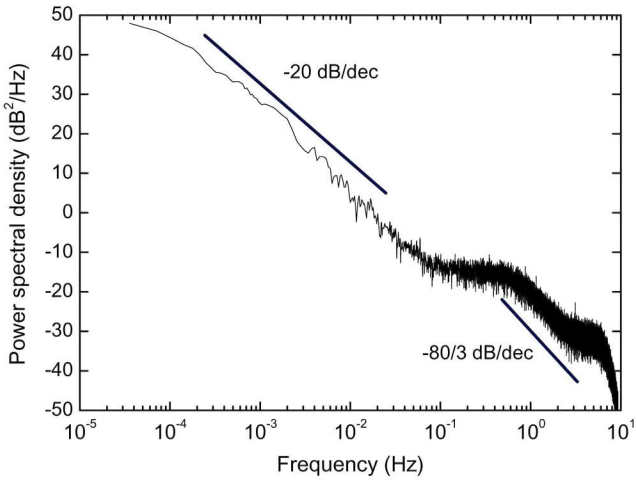

Fig. 1. Average power spectrum for a set of eight rain events recorded in May 2000.

During rain, the signal-to-noise power ratio of scintillation ρ_s must be carefully considered as measurements are not reliable beyond a certain attenuation value, due to the receiver noise. ρ_s has been calculated as indicated in [8], using the receiver carrier to noise power spectral density ratio C/N_0 of 59 dBHz in clear sky conditions [11]. From the calculations, it is found that ρ_s is higher than 10 dB for attenuation up to 12 dB.

III. Theoretical Considerations

Most of the studies on wet scintillation agree that scintillation intensity is highly correlated with rain attenuation. The main physical mechanism explaining this relationship is the increment in tropospheric turbulence during rainy periods.

The statistical dependence of scintillation intensity σ_χ on the simultaneous rain attenuation A has been modeled using different expressions. Matricciani *et al.* [17] showed theoretically that scintillation intensity is linked to rain attenuation by a power law. On the other hand, both Mertens *et al.* [6] and van de Kamp [7], working in the Ku and Ka-bands, found empirically a linear relationship between these two parameters.

Although the physical mechanisms are somewhat different, the statistical properties of wet scintillation can be derived from similar distributions to the ones used for clear air, but considering explicitly the rain-induced fade level [6]. This is the approach taken in this paper. In Section IV, the short-term PDF of scintillation amplitude, conditioned to a given rain fade level, is modeled by a Gaussian distribution, as proposed in the Mousley–Vilar model [3]. Nevertheless, a negative skewness is expected for strong intensities, with negative deviations being larger than positive deviations [18]–[21]. The long-term PDF of scintillation intensity, also dependent on the attenuation level, is fitted with lognormal distributions in Section V, as it is usually done in dry scintillation [3]. Finally, it should be possible to obtain the long-term PDF of scintillation amplitude by combining the two mentioned PDFs. This is checked against the data gathered in the experiment.

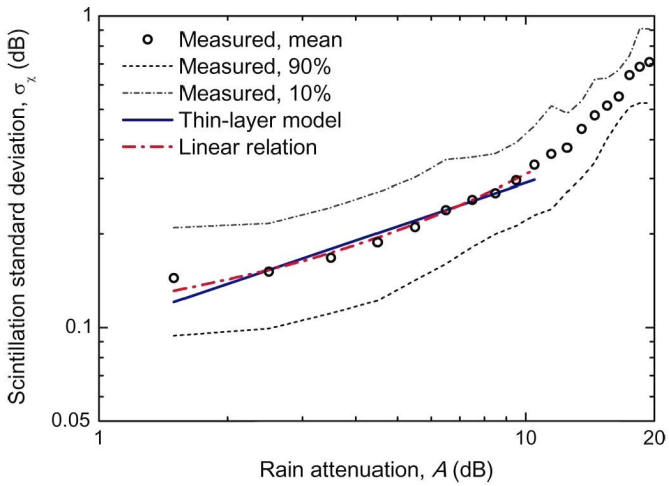

Fig. 2. Scintillation intensity, σ_χ, as a function of rain attenuation: mean and percentiles for 10% and 90%. Best fit with the thin layer model, (1), and a linear relationship, (2).

IV. Statistics of Scintillation Intensity

A. Relationship Between Attenuation and Scintillation Intensity

The experimental values of scintillation intensity have been classified according to simultaneous rain attenuation using 1 dB steps. It is important to note that the smallest attenuation values are not necessarily related to rain, but rather to clouds present before and after a precipitation event.

Fig. 2 shows the relation between attenuation and scintillation intensity. As expected, the higher the rain attenuation the higher the scintillation intensity. The increment of intensity is not quite significant for attenuations up to 2–3 dB, as part of the measured scintillation is actually due to turbulence inside the clouds, with no precipitation. In fact, the mean intensity value in the 1–2-dB interval, 0.145 dB, is very close to the mean value of dry scintillation, 0.139 dB [10]. The change of slope around 10–12 dB may indicate the increasing effect of system noise on the measurements.

The various types of relationships between rain attenuation and scintillation intensity introduced in Section III have been tested. For this purpose, only the range 1–10 dB, where the signal-to-noise ratio ρ_s is high enough, is considered.

A power-law expression is proposed in the turbulent thin-layer model [17]. By fitting the experimental data, the following relationship between rain attenuation and mean scintillation intensity is obtained:

$$\sigma_\chi = 0.1002 \cdot A^{\frac{(5/12)}{0.9}} \text{ dB} \tag{1}$$

where the exponent is not the original 5/12 considered in [17] but a refined value later proposed in [8], (5/12)/0.9.

A linear relationship between scintillation intensity and attenuation also seems to be adequate to fit the experimental data, leading to the following equation:

$$\sigma_\chi = 0.0210 \cdot A + 0.0997 \text{ dB}. \tag{2}$$

Expressions (1) and (2) are plotted in Fig. 2. It is clearly shown that they both can be used to estimate the mean scintillation intensity for attenuation up to 10 dB, which is the maximum value used in [7] and [8] when performing similar regression analysis. Nevertheless, the linear relationship is slightly better in terms of RMS error, as shown in Table I.

TABLE I
Mean and RMS Errors of Fitting Expressions (1) and (2) With the Experimental Data. Attenuation Range 1–10 dB

Fitting equation	Mean error (dB)	RMS error (dB)
Power law, (1)	$2 \cdot 10^{-4}$	$1.12 \cdot 10^{-2}$
Linear, (2)	$1.6 \cdot 10^{-3}$	$6.2 \cdot 10^{-3}$

B. Long-Term Distribution of Scintillation Intensity

The final objective of this section is to determine and model the PDF of scintillation intensity for all rainy periods $p(\sigma_\chi)$. Due to the close relationship between rain attenuation and scintillation, the first step is the analysis of the conditional distributions $p(\sigma_\chi \mid A)$.

Fig. 3 shows two examples of conditional distributions: for rain attenuation between 4 and 5 dB, and for rain attenuation between 8 and 9 dB. In both cases, a lognormal distribution seems to provide a good fitting to the data, which can be extended to other attenuation ranges. The more complex Gamma distribution, proposed by Karasawa *et al.* to model dry scintillation [4], has also provided a good performance although, in order to simplify the analysis, it will not be considered further in this paper.

The parameters mean σ_m and standard deviation σ_σ of the associated normal distribution of $\ln(\sigma_\chi)$ are collected in Table II. The mean value increases with attenuation, while it is the opposite for the standard deviation. A linear fitting of both parameters leads to the following equations:

$$\sigma_m = 0.0987 \cdot A - 2.156 \tag{3}$$

$$\sigma_\sigma = -0.0112 \cdot A + 0.346 \tag{4}$$

with the mean errors being $-3.1 \cdot 10^{-4}$ and $-2 \cdot 10^{-5}$ for (3) and (4), respectively, and the RMS errors 0.0306 and 0.0108 for (3) and (4), respectively.

The overall PDF of scintillation intensity $p(\sigma_\chi)$ that includes all the rainy periods regardless the attenuation is shown in Fig. 4. Unlike Fig. 3, the ordinate is in logarithmic scale, which facilitates the visualization of the fitting curves. The lognormal fit to the whole set of measured data is not adequate, especially for scintillation intensities above 0.3 dB. Alternative distributions have been tested in the attempt to fit the empirical data. The best performance was found for a generalized extreme value (GEV) distribution, which is commonly used in other engineering applications, as shown in [22] and [23]. The PDF of the GEV fit is given by the following:

$$p(\sigma_\chi) = \frac{1}{\alpha}\left[1 + \kappa\left(\frac{\sigma_\chi - \mu}{\alpha}\right)\right]^{-1-\frac{1}{\kappa}} e^{-(1+\kappa(\frac{\sigma_\chi-\mu}{\alpha}))^{\frac{1}{\kappa}}} \tag{5}$$

where μ is the location parameter, α the scale parameter, and κ the shape parameter. The best fitting values of these parameters are indicated in Fig. 4. They are link dependent and, without further experimental measurements at different conditions, it is not feasible to relate them to the physical characteristics of the Earth–satellite link.

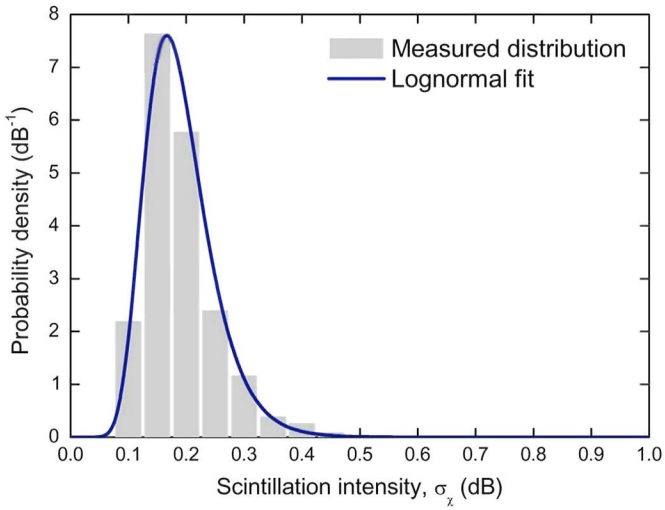

(a)

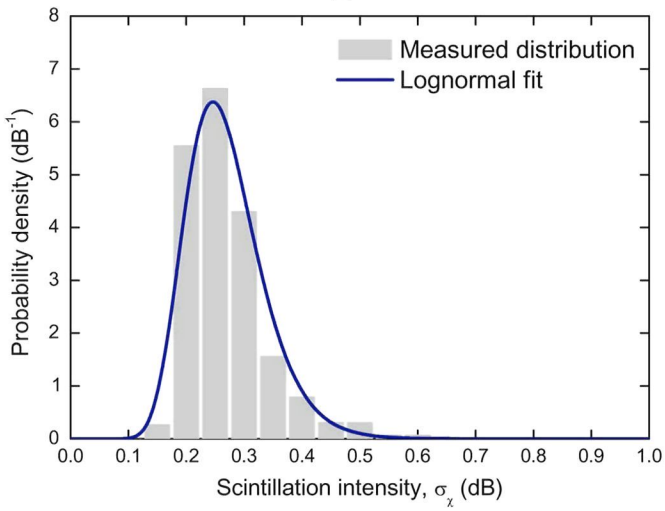

(b)

Fig. 3. Measured probability distributions of scintillation intensity conditioned to a mean attenuation $p(\sigma_\chi|A)$ and lognormal fits. (a) Rain attenuation: 4–5 dB. (b) Rain attenuation: 8–9 dB.

TABLE II
PARAMETERS OF THE LOGNORMAL FITTING TO THE CONDITIONAL PROBABILITY DENSITY FUNCTIONS $p(\sigma_\chi|A)$

Rain attenuation, A (dB)	Mean value of $\ln(\sigma_\chi)$, σ_m	Standard deviation of $\ln(\sigma_\chi)$, σ_σ
2 – 3	-1.932	0.309
3 – 4	-1.834	0.301
4 – 5	-1.705	0.300
5 – 6	-1.595	0.284
6 – 7	-1.476	0.298
7 – 8	-1.369	0.263
8 – 9	-1.343	0.246
9 – 10	-1.256	0.227

As an alternative way, $p(\sigma_\chi)$ can be derived from the individual lognormal fits of $p(\sigma_\chi|A)$, with the set of parameters gathered in Table II. The procedure requires numerical integration:

$$p(\sigma_\chi) = \int_0^\infty p(\sigma_\chi|A)p(A)dA \qquad (6)$$

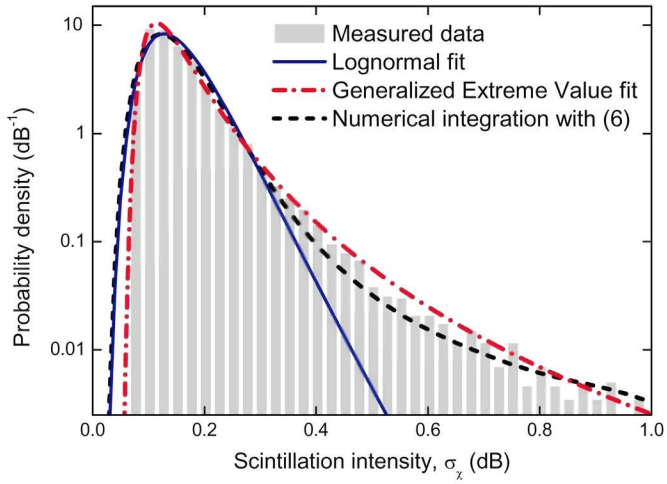

Fig. 4. PDF of $p(\sigma_\chi)$. Measured distribution, lognormal fit $(\sigma_m = -1.926, \sigma_\sigma = 0.373)$, generalized extreme value fit $(\mu = 0.123, \alpha = 0.037, \kappa = 0.285)$, and result of the numerical integration using (6).

where $p(A)$ is the experimental PDF of attenuation, which has been derived from the cumulative distribution [9]. The resulting curve, shown in Fig. 4, is very close to the experimental values. The performance is much better than when the lognormal distribution is used and similar to the one provided by the GEV distribution. From these results, it should be inferred that the long-term distribution of scintillation intensity $p(\sigma_\chi)$ is well characterized by (6), on the basis of a good parametrization of the conditioned distributions $p(\sigma_\chi|A)$.

V. STATISTICS OF SCINTILLATION AMPLITUDE

A similar approach to that used in the previous Section is followed when considering the statistics of scintillation amplitude χ. First, conditional distributions $p(\chi|\sigma_\chi)$ are analyzed. Then, the complete distribution of amplitude $p(\chi)$ is presented and compared with a numerical integration of the conditional distributions.

A. PDF of Amplitude Conditioned on the Scintillation Intensity

The short-term signal fluctuations due to clear-air tropospheric scintillation are usually assumed to follow a Gaussian distribution characterized only by the standard deviation σ_χ [3]. Using the measured data, the hypothesis of Gaussian distributions for the PDF of $p(\chi|\sigma_\chi)$ has been tested.

Two examples of these PDFs are presented in Fig. 5, corresponding to moderate intensities (σ_χ between 0.2 and 0.25 dB) and strong intensities (σ_χ between 0.75 and 0.8 dB). The first case exhibits small fluctuations and the normal fitting is completely satisfactory. In the second curve, the normal fitting works adequately for fluctuations up to ±2 dB, but beyond this point, experimental data depart from the normal distribution as fades are more frequent than the predicted values. This kind of behavior is equivalent to the asymmetry of short-term signal level fluctuation observed in dry scintillation [18]–[21]. In our case, the remains of rain attenuation components in the high-pass filtered signal may be partially responsible for it. An attempt has been made to test the asymmetrical scintillation model proposed in [24], which is based on a Rice–Nakagami

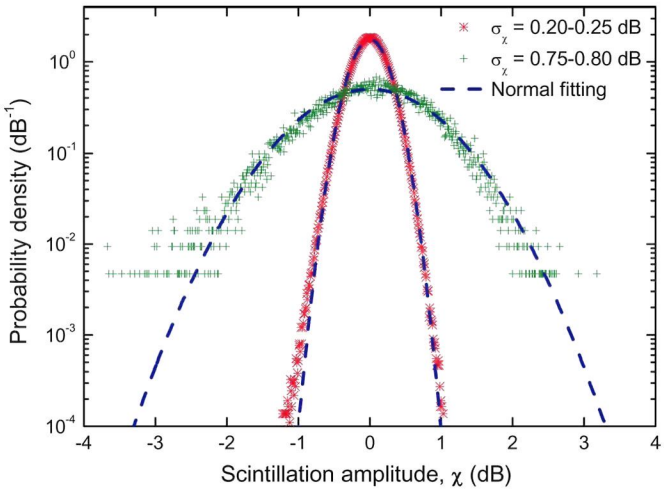

Fig. 5. Examples of PDFs of scintillation amplitude conditioned to intensity $p(\chi|\sigma_\chi)$.

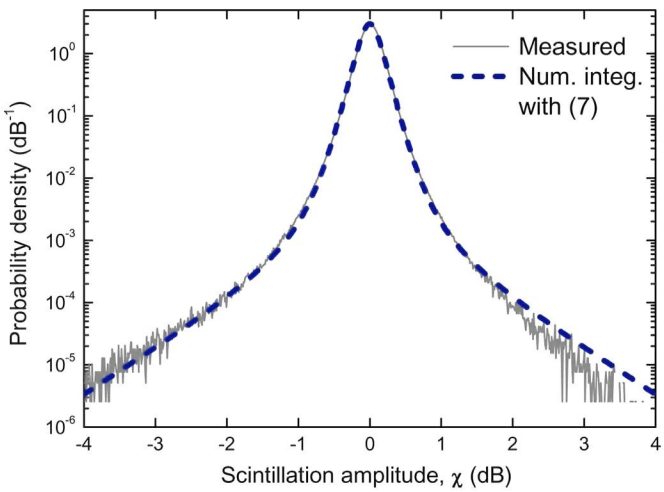

Fig. 6. PDF of scintillation amplitude, $p(\chi)$. Measured distribution and result of numerical integration using (7).

distribution for the short-term variations of electric field amplitude, but the measured asymmetry is too weak to infer any conclusion.

It can be said, in general, that short-term fluctuations due to both dry and wet scintillation can be well modeled by a normal distribution. The characterization can be improved by considering the skewness of the distribution for strong intensities, which are likely to be more frequent when simultaneous precipitation occurs.

B. Long-Term PDF of Scintillation Amplitude

The PDF of the measured scintillation amplitude $p(\chi)$ for all the rain events is shown in Fig. 6. The distribution is slightly asymmetrical, which is observable only for fluctuations higher than ±2 dB. This was expected from the results discussed in the previous section.

Following a similar analysis to that performed for σ_χ, the next step is to prove that the long-term PDF of χ can also be obtained from numerical integration of the conditional distributions. The following three assumptions are made. First, $p(\chi|\sigma_\chi)$ follows a normal distribution of zero mean and standard deviation σ_χ. Second, σ_χ is highly dependent on the rain attenuation level; specifically, $p(\sigma_\chi|A)$ are lognormal functions with parameters σ_m and σ_s defined in (3) and (4). Finally, $p(A)$ is the measured long-term PDF of rain attenuation. Then, the following iterated integral is derived:

$$p(\chi) = \int_0^\infty p(\chi|\sigma_\chi) \left[\int_0^\infty p(\sigma_\chi|A)p(A)dA \right] d\sigma_\chi. \qquad (7)$$

As seen in Fig. 6, the PDF of scintillation amplitude estimated with (7) is in very good agreement with the measured distribution.

In order to apply this methodology to the determination of the long-term distribution of scintillation amplitude, the following considerations must be taken into account. First, if $p(A)$ has not been empirically obtained, it can be derived from a rain attenuation prediction model, like the one proposed by ITU-R [5]. This distribution is usually considered to be lognormal [25]. Second, the lognormal parameters of the conditional distributions $p(\sigma_\chi|A)$, collected in (3)–(4) and in Table II, are link specific and are not directly applicable to other frequencies or elevation angles. Although equivalent equations have been derived in other experiments at lower frequencies [7], [8], more effort is needed to characterize the mean and standard deviation of the lognormal distributions.

VI. Conclusion

Dry and wet scintillation share several common characteristics. In general, amplitude fluctuations due to wet scintillation are stronger; however, some of the short-term distributions normally used for dry scintillation are also applicable when rain attenuation is present. Nevertheless, due to the high dependence of wet scintillation on link attenuation, it is not feasible to characterize it without explicitly considering the rain fade level. Therefore, distributions conditioned to the rain attenuation level must be used.

Propagation data gathered in the course of a V-band experiment have been used to characterize these phenomena. The empirical relationship between scintillation intensity and rain attenuation has been fitted to several regression curves. Both the power law proposed in the thin-layer model and the linear relationship perform quite well in the attenuation range 1–10 dB.

The PDFs of scintillation intensity conditioned to a given rain attenuation value are well fitted by lognormal distributions, as in the case of dry scintillation. But considering all the rainy periods, the overall PDF of scintillation intensity departs significantly from the lognormal, being very well fitted by a GEV distribution. Alternatively, it can be calculated from the lognormal conditioned distributions.

The short-term statistics of the fast fluctuations during rain also have common aspects with dry scintillation. In particular, the PDFs conditioned to a given scintillation intensity are normal, although significant skewness is observed for the strongest intensities, which is also usual in the absence of rain.

A set of expressions have been presented that allows to derive numerically the overall PDF of scintillation amplitude $p(\chi)$. The lognormal parameters, mean and standard deviation, of the conditional distributions of scintillation intensity $p(\sigma_\chi|A)$ must

be obtained in first place. The values of these parameters are given in Section IV for the conditions of this experiment; more research is needed to characterize their dependence on climate, frequency, or elevation angle. Then, the PDF of rain attenuation $p(A)$ is to be obtained from measurements or from prediction models. This process usually requires converting cumulative distributions (CDFs), which are most frequently used in this field, into probability distributions (PDFs). Finally, normal distributions can be assumed for the conditional PDFs of scintillation amplitude, $p(\chi|\sigma_\chi)$, although a more accurate approach could consider skewed distributions. The PDF $p(\chi)$ is then obtained from these three input functions, using numerical tools. This method provided excellent results when compared with the data measured in the experiment.

A good knowledge of the relationship between scintillation and rain attenuation is needed to calculate the combined effect of these two phenomena. Although rain attenuation is usually the dominant factor in the Earth–space path, an extra fade margin is required to compensate for amplitude fluctuations due to scintillation in the presence of precipitation. In this regard, the results presented in this paper can be used to estimate the cumulative distribution of total attenuation, and to improve the channel capacity through a better operation of systems during rain events.

References

[1] G. Brussaard and P. A. Watson, *Atmospheric Modelling and Millimetre Wave Propagation*. London, U.K.: Chapman & Hall, 1995.

[2] "Radiowave propagation modelling for SATCOM services at Ku-Band and above," ESA Publications Div., ESTEC, Noordwijk, The Netherlands, Final Rep., COST 255, , 2002.

[3] T. J. Moulsley and E. Vilar, "Experimental and theoretical statistics of microwave amplitude scintillations on satellite down-links," *IEEE Trans. Antennas Propag.*, vol. AP-30, no. 6, pp. 1099–1106, 1982.

[4] Y. Karasawa, M. Yamada, and J. E. Allnutt, "A new prediction method for tropospheric scintillation on Earth-space paths," *IEEE Trans. Antennas Propag.*, vol. 36, no. 11, pp. 1608–1614, 1988.

[5] *Propagation Data and Prediction Methods Required for the Design of Earth-Space Telecommunication Systems*, ITU-R Rec. P.618-10, ITU, Geneva, Switzerland, 2009.

[6] D. Mertens and D. Vanhoenacker-Janvier, "Rain fade dependence model of long-term scintillation amplitude distribution at 12.5 GHz," *Electron. Lett.*, vol. 37, no. 10, pp. 657–658, 2001.

[7] M. van de Kamp, "Climatic radiowave propagation models for the design of satellite communication systems" Ph.D. dissertation, Eindhoven Univ. of Technol., Eindhoven, The Netherlands, 1999 [Online]. Available: http://alexandria.tue.nl/extra2/9903235.pdf

[8] E. Matricciani and C. Riva, "18.7 GHz tropospheric scintillation and simultaneous rain attenuation measured at Spino d'Adda and Darmstadt with Italsat," *Radio Sci.*, vol. 43, pp. 1–13, 2008.

[9] P. Garcia-del-Pino, J. M. Riera, and A. Benarroch, "Slant path attenuation measurements at 50 GHz in Spain," *IEEE Antennas Wireless Propag. Lett.*, vol. 4, pp. 162–164, 2005.

[10] P. Garcia-del-Pino, J. M. Riera, and A. Benarroch, "Measurements of tropospheric scintillation on millimetre-wave satellite link," *Electron. Lett.*, vol. 43, no. 22, 2007.

[11] J. M. Riera, K. Al-Ansari, P. Garcia-del-Pino, and J. L. Besada, "Low-cost millimetric beacon receiver including total-power radiometer: Design, implementation and measurement calibration," *IEEE Antennas Propag. Mag.*, vol. 44, no. 1, pp. 45–54, 2002.

[12] E. Matricciani, M. Mauri, and C. Riva, "Polarization independence of tropospheric scintillation in clear sky: Results from Olympus experiment at Spino D'Adda," *IEEE Trans. Antennas Propag.*, vol. 46, no. 9, pp. 1400–1402, 1998.

[13] M. van de Kamp, J. K. Tervonen, E. T. Salonen, D. Vanhoenacker-Janvier, H. Vasseur, and G. Ortgies, "Polarisation independence of amplitude scintillation," *Electron. Lett.*, vol. 32, no. 18, p. 1650, 1996.

[14] E. Matricciani, "Physical-mathematical model of the dynamics of rain attenuation with application to power spectrum," *Electron. Lett.*, vol. 30, no. 6, pp. 522–524, 1994.

[15] V. I. Tatarski, *Wave Propagation in a Turbulent Medium*. New York: McGraw-Hill, 1961.

[16] E. Matricciani, M. Mauri, and C. Riva, "Scintillation and simultaneous rain attenuation at 49.5 GHz," presented at the 9th Int. Conf. Antennas Propag., Eindhoven, The Netherlands, Apr. 1995.

[17] E. Matricciani, M. Mauri, and C. Riva, "Relationship between scintillation and rain attenuation at 19.77 GHz," *Radio Sci.*, vol. 31, no. 2, pp. 273–279, 1996.

[18] O. Banjo and E. Vilar, "Measurement and modeling of amplitude scintillations on a low elevation Earth-space path and impact on communication systems," *IEEE Trans. Commun.*, vol. 34, no. 8, pp. 777–780, 1986.

[19] I. E. Otung, "Prediction of tropospheric amplitude scintillation on a satellite link," *IEEE Trans. Antennas Propag.*, vol. 44, no. 12, pp. 1600–1608, 1996.

[20] M. van de Kamp, "Experimental verification of asymmetrical short-term scintillation distribution model," *Electron. Lett.*, vol. 36, no. 7, pp. 663–664, 2000.

[21] I. E. Otung and B. G. Evans, "Short term distribution of amplitude scintillation on a satellite link," *Electron. Lett.*, vol. 31, no. 16, p. 1328, 1995.

[22] S. Kotz and S. Nadarajah, *Extreme Value Distributions: Theory and Applications*. London, U.K.: Imperial College Press, 2000.

[23] E. Castillo, A. S. Hadi, N. Balakrishnan, and J. M. Sarabia, *Extreme Value and Related Models With Applications in Engineering and Science*. Hoboken, NJ: Wiley, 2005.

[24] M. van de Kamp, "Asymmetric signal level distribution due to tropospheric scintillation," *Electron. Lett.*, vol. 34, no. 11, pp. 1145–1146, 1998.

[25] T. Maseng and P. M. Bakken, "A stochastic dynamic model of rain attenuation," *IEEE Trans. Commun.*, vol. 29, no. 5, pp. 660–669, 1981.